ISBN: 978-3-95450-236-3 ISSN: 2673-5350 doi:10.18429/JACoW-IBIC2023-WEP035

STATISTICAL PROPERTIES OF SCHOTTKY SPECTRA

C. Lannoy[1,*], D. Alves, K. Lasocha, N. Mounet, CERN, Geneva, Switzerland
T. Pieloni, EPFL, Lausanne, Switzerland
[1]also at EPFL, Lausanne, Switzerland

Abstract

Schottky signals are used for non-invasive beam diagnostics as they contain information on various beam and machine parameters. The instantaneous Schottky signal is, however, only a single realisation of a random process, implicitly depending on the discrete distribution of synchrotron and betatron amplitudes and phases among the particles. To estimate the expected value of the Schottky power spectrum, and reveal the inner structure of the Bessel satellites described by the theory, the averaging of instantaneous Schottky spectra is required. This study describes this procedure quantitatively by analysing the statistical properties of the Schottky signals, including the expected value and variance of Schottky power spectra. Furthermore, we investigate how these quantities evolve with the number of particles in the bunch, the observed harmonic of the revolution frequency, the distribution of synchrotron oscillation amplitudes, and the bunch profile. The theoretical findings are compared against macro-particle simulations as well as Monte Carlo computations.

INTRODUCTION

The Large Hadron Collider (LHC) Schottky system provides a single spectrum every second, based on the signal acquired over approximately the last 16 000 revolutions. Notably, consecutive spectra exhibit significant dissimilarity, requiring the aggregation of numerous spectra to attain the mean value. This study aims at exploring the inherent variability of consecutive instantaneous Schottky spectra and at characterising their statistical properties.

The LHC Schottky monitors measure the power spectral density (PSD) of a signal (intensity for the longitudinal spectrum, or dipole moment for the transverse one). For a random process $X(t)$, the PSD is defined in general by [1, Eq. (10.9)]

$$P(\omega) = \lim_{T\to\infty} \frac{1}{2T}|X_T(\omega)|^2, \tag{1}$$

where $X_T(\omega)$ is the Fourier transform of the truncated process

$$X_T(\omega) = \int_{-T}^{T} X(t)e^{-j\omega t}dt.$$

In these proceeding we will first investigate the statistical properties of the longitudinal spectrum, before elaborating on the transverse one. Then we will compare our results with simulations and the available measurements, and finally present our conclusions.

* christophe.lannoy@cern.ch

LONGITUDINAL SCHOTTKY SPECTRA

As shown in the literature [2–5], the intensity signal $i(t)$ of a bunch consisting of N particles can be written

$$i(t) = qf_0 \sum_{i=1}^{N} \sum_{n,p=-\infty}^{\infty} J_p(n\omega_0\widehat{\tau_i})\, e^{j(n\omega_0 t + p\Omega_{s_i} t + p\varphi_{s_i})}, \tag{2}$$

where J_p is the Bessel function of the first kind of order p, q the charge of the particle, $f_0 = \omega_0/2\pi$ the revolution frequency, and $\widehat{\tau_i}$, Ω_{s_i}, and φ_{s_i}, respectively, the synchrotron time amplitude[1], frequency, and initial phase of particle i. The summations over n and p are related to the revolution frequency harmonic and the Bessel satellite number p.

Equation (2) is a deterministic signal entirely defined by a set of N amplitudes $\widehat{\tau}_i$ and N phases φ_{s_i} (the synchrotron frequencies Ω_{s_i} can be determined from the synchrotron amplitudes as in [6, 7]). To examine the statistical properties of the Schottky spectra, we define the corresponding random process $I(t)$ of the intensity signal $i(t)$

$$I(t) = qf_0 \sum_{i,n,p} J_p(n\omega_0\widehat{T}_i)\, e^{j(n\omega_0 t + p\Omega_{s_i} t + p\Phi_{s_i})}, \tag{3}$$

where the summation bounds have been omitted for readability. The random variables $\widehat{T}_i$ and Φ_{s_i} describe respectively, the synchrotron time amplitude and initial phase for particle i. Equation (2) can be seen as one realisation of the random process defined by Eq. (3).

In the following, Φ_{s_i} is assumed to follow a uniform distribution on $[0, 2\pi]$, while $\widehat{T}_i$ is described by various probability density functions $g(\widehat{\tau})$, such as the Rice distribution as in [7]

$$g(\widehat{\tau}) = \frac{\widehat{\tau}}{\sigma^2} e^{-\frac{\widehat{\tau}^2}{2\sigma^2} - \frac{b^2}{2}} I_0(\widehat{\tau}b/\sigma),$$

or a distribution corresponding to a Gaussian bunch profile

$$g(\widehat{\tau}) = \frac{\widehat{\tau}}{\sigma^2} e^{-\frac{\widehat{\tau}^2}{2\sigma^2}},$$

in order to assess the impact of different bunch profiles.

Applying the PSD definition from Eq. (1) to Eq. (3) yields [8]

$$P(\omega) = q^2 f_0^2 \sum_{\substack{i,n,p \\ i',p'}} J_p(n\omega_0\widehat{T}_i) J_{p'}(n\omega_0\widehat{T_{i'}}) e^{j(p\Phi_{s_i} - p'\Phi_{s_{i'}})} \times 2\pi\delta\left(n\omega_0 + p\Omega_{s_i} - \omega\right)\delta_K\left(p\Omega_{s_i} - p'\Omega_{s_{i'}}\right), \tag{4}$$

[1] By time amplitude, we mean the maximum time arrival difference between a given particle and the synchronous particle

ISBN: 978-3-95450-236-3 ISSN: 2673-5350 doi:10.18429/JACoW-IBIC2023-WEP035

where δ is the Dirac delta distribution and with

$$\delta_K(x) = \lim_{T\to\infty} \frac{\sin(xT)}{xT} = \begin{cases} 1, & \text{if } x = 0, \\ 0, & \text{otherwise.} \end{cases}$$

Central Satellite

The power (i.e. the integrated PSD) of the central satellite $p = 0$, at a given harmonic $n = n_h$ can be deduced from Eq. (4) and is given by

$$\begin{aligned} P_{(0)} &= q^2 f_0^2 \sum_{i=1}^{N}\sum_{i'=1}^{N} J_0(n_h\omega_0\widehat{T_i}) J_0(n_h\omega_0\widehat{T_{i'}}) \\ &= q^2 f_0^2 \left(\sum_{i=1}^{N} Z_i\right)^2, \end{aligned} \tag{5}$$

where we defined the random variables

$$Z_i = J_0(n_h\omega_0\widehat{T_i}), \qquad \forall i \in [1, N], \tag{6}$$

In the following we derive the expected power and variance of the central satellite.

Expected Power Using the linearity of the expectation and the fact that the expected value of a product is the product of the expected values for independent random variables, we have

$$\begin{aligned} \frac{E(P_{(0)})}{q^2 f_0^2} &= E\left(\sum_{i=1}^{N}\sum_{j=1}^{N} Z_i Z_j\right) \\ &= \sum_{i=1}^{N} E(Z_i^2) + \sum_{i=1}^{N}\sum_{\substack{j=1 \\ j\neq i}}^{N} E(Z_i)E(Z_j) \\ &= N\beta + N(N-1)\alpha^2, \end{aligned} \tag{7}$$

where we defined the notations

$$\alpha = E(Z_i), \qquad \beta = E(Z_i^2), \tag{8}$$

for the first and second moments of Z_i. These are independent of i since all the particles have the same synchrotron amplitude distribution. Note that if $\alpha \approx 0$, the dominant term of the expected value of the power for the central satellite, scales as N rather than N^2.

Variance The variance can be expressed as

$$Var\left(P_{(0)}\right) = E\left(P_{(0)}^2\right) - \left(E(P_{(0)})\right)^2, \tag{9}$$

where the second term is the square of the average power calculated in Eq. (7). From the multinomial theorem, the first term can be expanded using

$$E\left[\left(\sum_{i=1}^{N} Z_i\right)^4\right] = \sum_{\substack{k_1+k_2+\ldots+k_N=4 \\ k_1,k_2,\ldots,k_N\geq 0}} \frac{4!}{k_1!k_2!\ldots k_N!} E\left[\prod_{i=1}^{N} Z_i^{k_i}\right], \tag{10}$$

where the sum is taken over all combinations of non-negative integer indices k_1 through k_N.

Substituting Eqs. (7) and (10) in Eq. (9), we obtain the variance of the power for the central satellite [8]

$$\begin{aligned} \frac{Var\left(P_{(0)}\right)}{q^4 f_0^4} &= N\delta + (4N^2 - 4N)\gamma\alpha + (2N^2 - 3N)\beta^2 \\ &+ (4N^3 - 16N^2 + 12N)\beta\alpha^2 + (-4N^3 + 10N^2 - 6N)\alpha^4, \end{aligned} \tag{11}$$

where γ and δ represent the third and fourth moments of Z_i.

It is worth noting that Eq. (5) is formally identical to the squared distance of a one-dimensional random walk of N steps of variable length Z_i. By reducing Eq. (5) to the particular case of unit steps, we have $\alpha = \gamma = 0$, $\beta = \delta = 1$, and we find the same expression for the mean and variance as in the one-dimensional random walk of unit steps [9].

Non-Central Satellites

For non-central satellites (i.e. $p \neq 0$), we extend the notation introduced in Eq. (6) to different order p of the Bessel function

$$Z_{i,(p)} = J_p(n_h\omega_0\widehat{T_i}), \qquad \forall i \in [1, N].$$

Similarly, we also define the following moments of $Z_{i,(p)}$

$$\beta_{(p)} = E(Z_{i,(p)}^2), \qquad \delta_{(p)} = E(Z_{i,(p)}^4). \tag{12}$$

The power contained in a given satellite p, can be derived from Eq. (4) and is given by [8]

$$\begin{aligned} P_{(p)} &= q^2 f_0^2 \sum_{i,i'} J_p(n_h\omega_0\widehat{T_i}) J_p(n_h\omega_0\widehat{T_{i'}}) e^{jp(\Phi_{s_i} - \Phi_{s_{i'}})} \\ &= q^2 f_0^2 \left|\sum_i Z_{i,(p)} e^{jp\Phi_{s_i}}\right|^2. \end{aligned} \tag{13}$$

By assuming that $\widehat{T_i}$ and Φ_{s_i} are independent random variables, one can show that the expected value and variance[2] for non-central satellites are respectively given by [8]

$$\begin{aligned} E(P_{(p)}) &= q^2 f_0^2\, N\beta_{(p)}, \\ Var(P_{(p)}) &= q^4 f_0^4 \left(N\delta_{(p)} + (N^2 - 2N)\beta_{(p)}^2\right). \end{aligned}$$

Note that Eq. (13) is formally identical to the squared distance of a two-dimensional random walk of N steps of variable length $Z_{i,(p)}$ and directions $p\Phi_{s_i}$. By reducing Eq. (13) to the particular case of unit steps, we have $\beta_{(p)} = \delta_{(p)} = 1$, and we find the same expression for the mean and variance as in the two-dimensional random walk of unit steps [10].

Figure 1 illustrates the coefficient of variation (CV), defined for both central ($p = 0$) and non-central satellites as

$$CV_{(p)} = \frac{\sqrt{Var(P_{(p)})}}{E(P_{(p)})}.$$

As can be seen, for typical LHC conditions, CV is $\sqrt{2}$ for the central satellite and 1 for non-central satellites.

[2] The variance was derived under the assumption of a linear RF bucket.

ISBN: 978-3-95450-236-3 ISSN: 2673-5350 doi:10.18429/JACoW-IBIC2023-WEP035

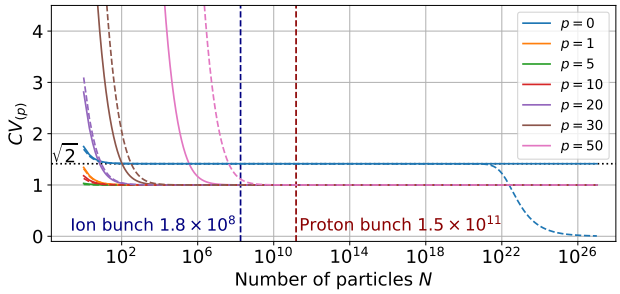

Figure 1: CV of the longitudinal satellites around the harmonic $n_h = 427\,725$ for a Rice amplitude distribution (dashed lines, $\sigma_r = 0.22$ ns and $b_r = 1.306$) and a Gaussian bunch profile (solid lines, $\sigma_g = 0.31$ ns).

TRANSVERSE SCHOTTKY SPECTRA

The transverse Schottky spectrum is given by the power spectral density of the dipole moment signal. By assuming that chromaticity $Q\xi$ is the only source of betatron frequency spread, the corresponding random process of the dipole moment can be written [2, 5]

$$D(t) = \sum_{(\pm)} \sum_{i=1}^{N} \sum_{n,p=-\infty}^{\infty} \frac{\widehat{X}_i q f_0}{2} J_p\left(\chi^{\pm}_{\widehat{T}_i, n\mp Q_I}\right) \times e^{j\left(t[(n\pm Q_F)\omega_0 + p\Omega_{s_i}] \pm \Phi_{\beta_i} + p\Phi_{s_i}\right)},$$

where the nominal tune is decomposed into its integer and fractional part $Q = Q_I + Q_F$ and with

$$\chi^{\pm}_{\widehat{T}_i, n} = \left(n \pm \frac{Q\xi}{\eta}\right)\omega_0 \widehat{T}_i.$$

In the above equations, η is the slippage factor, and $\widehat{X}_i$, Φ_{β_i} are respectively, the random variable of the amplitude, and the initial phase of the betatron motion of particle i. The summation over $\pm$ corresponds to the upper and lower transverse sidebands of the Schottky spectrum.

The PSD of the dipole moment can then be computed with Eq. (1), and the mean and variance of the power for a given satellite p around the Schottky harmonic $n = n_h$ can be derived, leading to the following expressions [8]:

$$E(P^{\pm}_{(p)}) = \frac{N q^2 f_0^2 \widehat{x_2}}{4} \beta^{\pm}_{(p)}, \tag{14}$$

$$Var\left(P^{\pm}_{(p)}\right) = \frac{q^4 f_0^4}{16}\left(N\widehat{x_4}\delta^{\pm}_{(p)} + (N^2 - 2N)\widehat{x_2}^2 (\beta^{\pm}_{(p)})^2\right),$$

with $\widehat{x_2}$ and $\widehat{x_4}$, the second and fourth moments of $\widehat{X}_i$, and where we extended the notations introduced previously with

$$\beta^{\pm}_{(p)} = E\left[J_p^2\left(\chi^{\pm}_{\widehat{T}_i, n_h\mp Q_I}\right)\right], \quad \delta(p)^{\pm} = E\left[J_p^4\left(\chi^{\pm}_{\widehat{T}_i, n_h\mp Q_I}\right)\right].$$

In contrast to the longitudinal spectrum, these expressions are also valid for the central transverse satellites due to the additional betatron phase appearing in the dipole moment. The CVs behave similarly to those of the longitudinal satellites, approaching 1 as N becomes sufficiently large (including the central satellites).

Figure 2 illustrates how the power of different Bessel satellites, as given by Eq. (14), are impacted by the harmonic number and the chromaticity on each sideband. It can be observed that as the harmonic number increases, the power of lower order satellites decreases, while the opposite occurs for higher order satellites. The effect of chromaticity can also be observed, resulting in a higher and narrower upper band compared to the lower band.

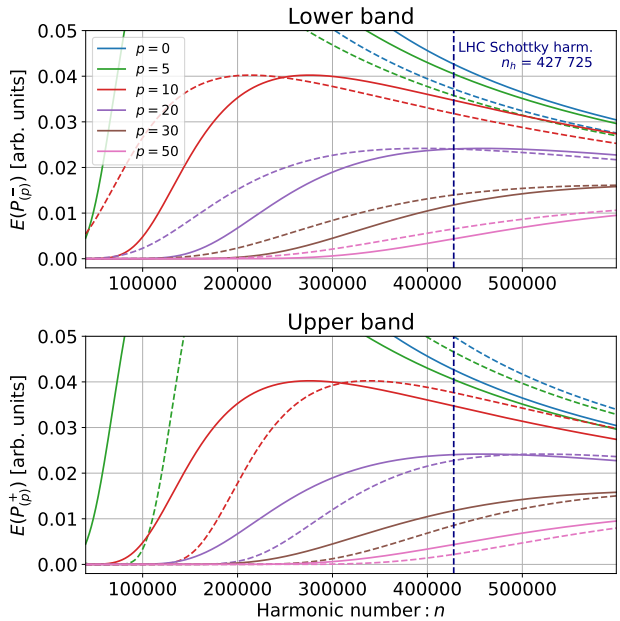

Figure 2: Harmonic scan of the expected powers of the transverse Bessel satellites for a Gaussian bunch profile ($\sigma_g = 0.31$ ns). The solid lines correspond to a zero chromaticity $Q\xi = 0$ while the dashed lines correspond to $Q\xi = 20$.

SIMULATIONS AND MEASUREMENTS

The theoretical equations derived in this study are compared against macro-particle and Monte-Carlo simulations of a realistic LHC ion fill in Fig. 3. The macro-particle simulations has been performed using PyHEADTAIL [11, 12] and the method used to retrieve the Schottky spectra from the tracking simulations is presented in [13]. The procedure of the Monte-Carlo simulation is described in [13, 14]. Both simulation techniques show a good agreement with the theoretical predictions and a clear convergence to a CV of $\sqrt{2}$ and 1 can be observed.

It should be noted that the previously developed theory is studying the mean and variance over different random draws of the bunches (phases and amplitudes of synchrotron and betatron motions), while in the real machine, there is a unique instance of the bunch. However, due to various non-linearities present in reality, the relative initial phases of synchrotron and betatron motions are drifting with time.

ISBN: 978-3-95450-236-3 ISSN: 2673-5350 doi:10.18429/JACoW-IBIC2023-WEP035

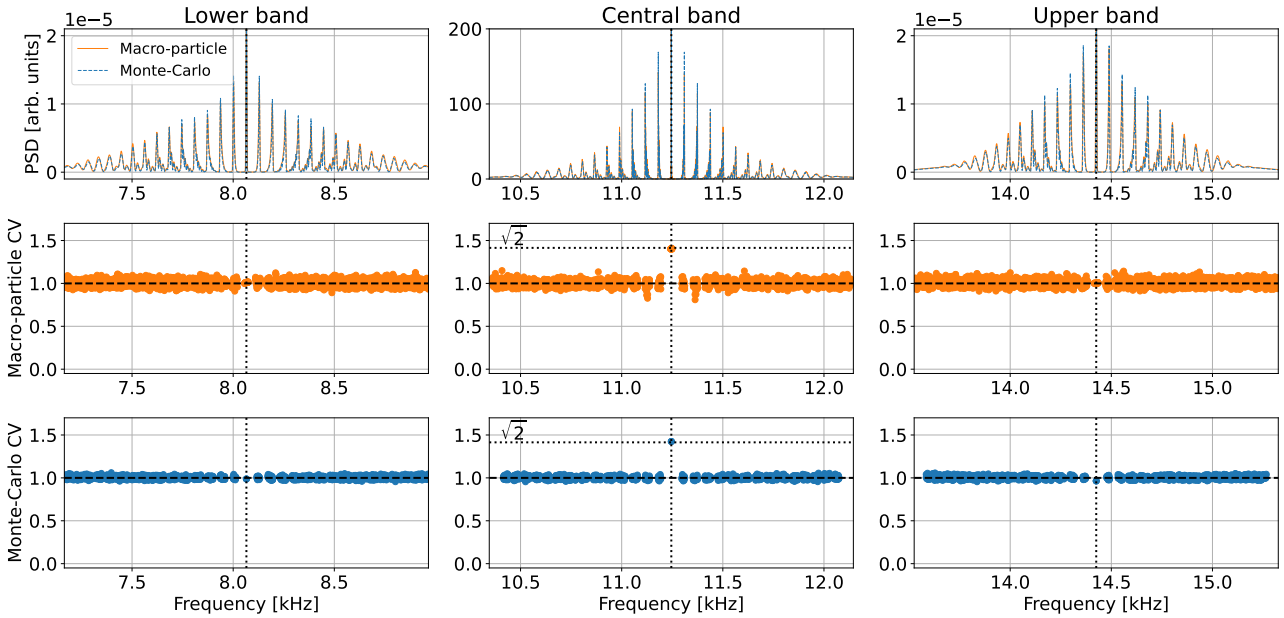

Figure 3: Macro-particle and Monte-Carlo simulations of a Schottky spectrum. The average spectrum and CV are based on 1000 random draws of the bunch for the macro-particle simulation, and 5000 random draws for the Monte-Carlo simulation.

After a given period, this unpredictable drift is equivalent to drawing new random phases, making the averaging over successive instantaneous Schottky spectra equivalent to the averaging over different random draws of the bunch. The same conclusion can not be drawn for the longitudinal central satellite, since the synchrotron phases do not appear in Eq. (5). Figure 4 presents an experimental measurement from the LHC Schottky monitors. The CV for the transverse sidebands and the non-central ($|p| > 2$) longitudinal satellites agree with the theory. No conclusion can be drawn for the central ($p = 0$) longitudinal satellite for the reason given above. The CVs for $p = \pm 1$ and ± 2 longitudinal satellites deviate from the predictions, which suggests that these satellites are subject to effects beyond the adopted theory of Schottky spectra and should not be used for diagnostics.

CONCLUSION

The aim of this study was to quantify the statistical properties of Schottky spectra and reveal the dependencies on particle count, harmonic number, and oscillation amplitude distribution. Our analysis demonstrated the convergence of the coefficient of variation to specific, non-zero values, for different Bessel satellites. This highlights the importance of averaging instantaneous Schottky spectra to access the mean spectrum described by existing theories. Our findings were validated through simulations and data from the LHC Schottky monitors and while transverse and non-central longitudinal satellites exhibit consistent convergence in the experimental data, the behaviour of the central longitudinal satellite still requires further investigation.

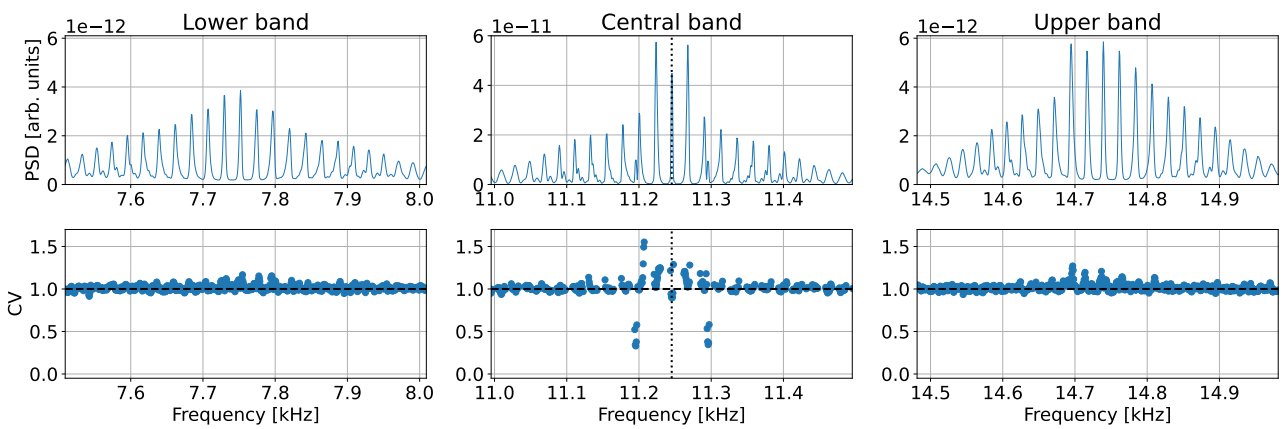

Figure 4: Experimental LHC Schottky spectrum taking during fill 8412 from '2022-11-18 17:44:00' to '2022-11-18 18:17:00'. Upper plots: average of 1980 instantaneous Schottky spectra. Lower plots: CV of the PSD.

ISBN: 978-3-95450-236-3 ISSN: 2673-5350 doi:10.18429/JACoW-IBIC2023-WEP035

REFERENCES

[1] S. L. Miller and D. Childers, *Probability and Random Processes (Second Edition)*. Academic Press, 2012. doi:10.1016/B978-0-12-386981-4.50013-8

[2] D. Boussard, "Schottky noise and beam transfer function diagnostics," p. 42, 1986. doi:10.5170/CERN-1987-003-V-2.416

[3] S. Chattopadhyay, "Some fundamental aspects of fluctuations and coherence in charged-particle beams in storage rings," *AIP Conference Proceedings*, vol. 127, no. 1, pp. 467–623, 1985. doi:10.1063/1.35175

[4] J. L. Laclare, "Bunched beam coherent instabilities," 1987. doi:10.5170/CERN-1987-003-V-1.264

[5] K. Lasocha, "Non-Invasive Beam Diagnostics with Schottky Signals and Cherenkov Diffraction Radiation," PhD thesis, Jagiellonian University, Kraków, Poland, 2022. https://cds.cern.ch/record/2846538

[6] D. Alves and K. Lasocha, "Kalman filter-based longitudinal phase-space reconstruction method for hadron machines," *Phys. Rev. Accel. Beams*, vol. 24, no. 9, p. 072 801, 2021. doi:10.1103/PhysRevAccelBeams.24.072801

[7] K. Lasocha and D. Alves, "Estimation of longitudinal bunch characteristics in the LHC using Schottky-based diagnostics," *Phys. Rev. Accel. Beams*, vol. 23, no. 6, p. 062 803, 2020. doi:10.1103/PhysRevAccelBeams.23.062803

[8] C. Lannoy, "Statistical properties of Schottky spectra," CERN note, in preparation.

[9] Random Walk–1-Dimensional. https://mathworld.wolfram.com/RandomWalk1-Dimensional.html

[10] J. M. Borwein, D. Nuyens, A. Straub, and J. Wan, "Some arithmetic properties of short random walk integrals," *The Ramanujan Journal*, vol. 26, no. 1, pp. 109–132, 2011. doi:10.1007/s11139-011-9325-y

[11] PyHEADTAIL code repository. https://github.com/PyCOMPLETE

[12] K. S. B. Li *et al.*, "Code development for collective effects," in *Proc. HB'16, Malmö, Sweden*, 2016, pp. 362–367. doi:10.18429/JACoW-HB2016-WEAM3X01

[13] C. Lannoy, D. Alves, N. Mounet, and T. Pieloni, "LHC Schottky Spectrum from Macro-Particle Simulations," in *Proc. IBIC'22*, Kraków, Poland, 2022, pp. 308–312. doi:10.18429/JACoW-IBIC2022-TUP34

[14] M. Betz, O. R. Jones, T. Lefevre, and M. Wendt, "Bunched-beam Schottky monitoring in the LHC," *Nucl. Instrum. Methods Phys. Res., A*, vol. 874, no. 14, pp. 113–126, 2017. doi:10.1016/j.nima.2017.08.045